Two-Dimensional Time-Frequency Ultrafast Infrared Vibrational Echo Spectroscopy

K. A. Merchant, David E. Thompson, and M. D. Fayer
Department of Chemistry, Stanford University, Stanford, California 94305
(Received 15 September 2000)

2D spectrally resolved ultrafast (<200 fs) IR vibrational echo experiments were performed on $Rh(CO)_2$acac [(acetylacetonato)dicarbonylrhodium (*I*)]. The 2D spectra display features that reflect the 0-1 and 1-2 transitions and the combination band transition of the symmetric (*S*) and antisymmetric (*A*) CO stretching modes. Three oscillations in the data arise from the frequency difference between the *S* and *A* modes (quantum beats) and the *S* and *A* anharmonicities. A new explanation is given for these "anharmonic" oscillations. Calculations show that spectral resolution enables the 0-1 and 1-2 dephasing to be measured independently.

DOI: 10.1103/PhysRevLett.86.3899 PACS numbers: 78.47.+p, 78.30.Jw

I. Introduction.—The development of pulsed NMR [1] and the extension to two-dimensional (2D) methods [2], has vastly expanded the usefulness of NMR in many areas of science. The advent of the photon echo, the electronic excited state equivalent of the spin echo [3], and ultrafast 2D photon echo experiments [4,5] have extended NMR-like techniques into the visible and the UV. Recently, photon echoes were extended to the study of molecular vibrations in condensed matter as ultrafast IR vibrational echoes [6]. Vibrational echoes [7–13] make possible the direct study of molecular structural degrees of freedom using the types of sensitive probes that have been available for the study of spins and electronic excited states.

In this Letter, 2D (time-frequency) ultrafast IR vibrational echo spectroscopy (VES) experiments are presented. The ultrashort pulses required to study vibrational dynamics [14] with vibrational echoes can have bandwidths that produce coherent excitation of multiple excited vibrational states resulting in complex oscillatory nonexponential decay curves even if each transition would give rise to a single exponential decay. By spectrally resolving the ultrafast vibrational echo and obtaining a 2D echo spectrum, the time resolution is preserved, the nature of the signal can be more readily elucidated, and additional information can be obtained. Spectrally resolved ultrafast VES is an addition to an increasing collection of new 2D ultrafast IR spectroscopic methods [10,11,15–18].

II. Experimental procedures.—The experiments [12] use mid-IR pulses centered at 2050 cm^{-1}, 180 fs in duration, and 90 cm^{-1} in bandwidth. The pulses were produced using an amplified Ti:sapphire pumped optical parametric amplifier. A 3.2 μJ pulse was split into two pulses having wave vectors $\vec{k}_1$ and $\vec{k}_2$ that were crossed and focused to a spot size of ~200 μm at the sample. The echo pulse emerged in the $2\vec{k}_2-\vec{k}_1$ direction. The second pulse was delayed by a time τ. Vibrational echo spectra (resolution 2 cm^{-1}) were measured by focusing the echo pulse into a 1 m scanning monochromator with a 150 lines/mm grating, and were recorded as a function of the excitation pulse delay.

The sample of (acetylacetonato)dicarbonylrhodium (*I*) [$Rh(CO)_2$acac] (Aldrich) in poly(methyl methacrylate) (PMMA) (Aldrich) was prepared under oxygen-free conditions by solvent (methylene chloride) evaporation in a vacuum desiccator for several days. The resulting high optical quality 300 μm thick film was mounted on a sample holder in a continuous flow cryostat. A silicon diode thermometer was bonded to the sample surface. Data were collected at 110 K [Fig. 1(a)] and 150 K [Fig. 1(b)]. IR spectra show that the peak positions are temperature independent. The symmetric (*S*) and antisymmetric (*A*) CO absorption lines are centered at 2082 cm^{-1} (FWHM = 12.8 cm^{-1}) and 2010 cm^{-1} (FWHM = 15.4 cm^{-1}), respectively.

III. Results and discussion.—There are six energy levels that are sampled in the experiment: the ground state, the *S* fundamental and overtone, the *A* fundamental and overtone, and the *S*-*A* combination band. Figure 1(a) displays VES data taken with low time resolution (500 fs per step). The inset shows the IR absorption spectrum. The higher energy VES band is from the *S* mode, and the lower frequency component is from the *A* mode. Each band has contributions from the ground state ($v = 0$) to first excited state ($v = 1$) transition and from the $v = 1$ state to the second excited state ($v = 2$, overtone) transition. The 1-2 contributions are on the red side of each band. Both features display oscillations at the frequency of the anharmonic shift, that is, the difference between the 0-1 and 1-2 transition frequencies (10.7 cm^{-1} for *S* and 13.7 cm^{-1} for *A*) [7,14]. The VES spectrum is background-free although there is significant solvent absorption in the linear IR spectrum (see inset). The ability of the VES coherent pulse sequence to eliminate unwanted absorptions [9,15] is akin to methods used in pulsed NMR to eliminate unwanted spectral features [19,20].

Figure 1(b) is a more detailed display of the *S* band. The time resolution is increased to 32 fs per step, and additional features are evident. The inset is a time slice of the data at 2084 cm^{-1}. The high frequency oscillations, which can be seen both in the main plot and in the inset, are at 71.1 cm^{-1}, the nominal splitting between the

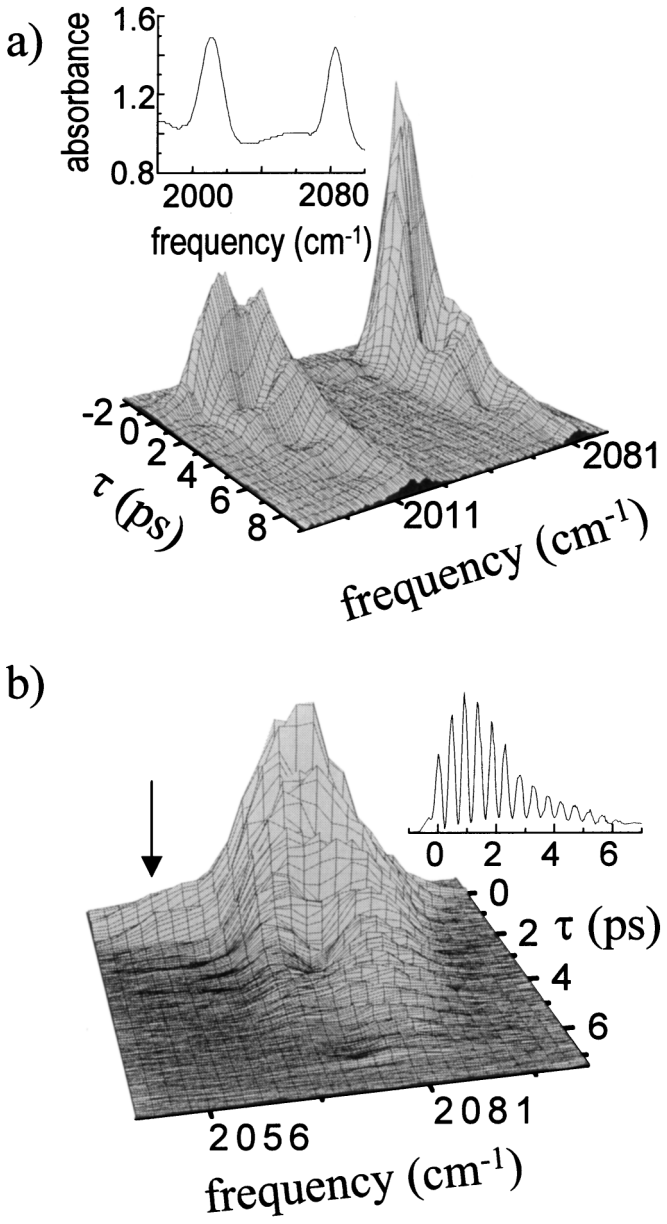

FIG. 1. 2D vibrational echo spectra of the two CD stretching modes in $Rh(CO)_2(acac)$. (a) Low time resolution showing both modes. The data show pronounced oscillations in the middle of each peak. The oscillation frequency is equal to the anharmonicity of the particular transition. The inset shows the IR spectrum of the sample. The broad solvent features at 1975 and 2050 cm^{-1} are absent in the vibrational echo spectrum. (b) High time resolution of the symmetric peak. The high frequency oscillations are at the difference in frequency between the two modes. The inset is a time cut at 2084 cm^{-1}. The smaller peak on the red side of the main band (arrow) is produced by the combination band transition and is shifted 25 cm^{-1}, reflecting the coupling between the two modes.

S and *A* modes. These oscillations are quantum beats arising because the transition is branching. A lower amplitude feature (marked with an arrow) is visible on the red side of the band. It arises from combination band transitions, that is, transitions in which both the *S* and *A* modes are excited. In linear spectroscopy, the combination band absorption occurs at ~4067 cm^{-1}, the sum of the *S* and *A* energies shifted by an amount (25 cm^{-1} to the red) that reflects the anharmonic coupling between the two modes. In the vibrational echo experiment, the combination band is accessed through excited state absorption [i.e., initial interaction at 2082 (2010) cm^{-1}, followed by an interaction at 1985 (2057) cm^{-1}], and appears as two peaks that are shifted to the red of each fundamental transition by 25 cm^{-1}. The decay of the spectrum reflects the homogeneous dephasing of the system. The 0-1 transition (blue side of the line) decays somewhat more slowly than the 1-2 transition (red side of the main band), and the combination band peak decays very quickly. A complete analysis of the dephasing linewidth will not be given here. However, we can estimate the decay time of the 0-1 and 1-2 levels to be ~2–3 ps, with corresponding pure dephasing linewidths of ~0.9–1.3 cm^{-1}, indicating that, at this temperature, the system is massively inhomogeneously broadened. Additionally, in a simple model, the decay of the combination band peak would be closely related to the homogeneous dephasing of the *S* and *A* modes. The rapid decay of the combination band peak suggests that fluctuations of the anharmonic coupling of the modes may play an important role in the dephasing.

The lower frequency anharmonic oscillations [Fig. 1(a) and 1(b)] are not normal quantum beats or other types of beats seen in coherence experiments on a variety of multilevel systems [21,22]. The origin of the oscillations is different from the one proposed previously for experiments without frequency resolution [7,23] and applies to experiments with and without spectral resolution. The current interpretation of the anharmonic oscillations is that distinct frequencies, the 0-1 and 1-2 frequencies that arise from distinct Feynman diagrams, interfere with each other [7]. The fact that oscillations are seen in the spectrally resolved VES data (2 cm^{-1} resolution) shows that this description of the process is incomplete.

A normal quantum beat requires a branching transition. The beat arises because there are pairs of diagrams in which the first interaction in one diagram takes the system to a state $|i\rangle$ and the first interaction in the second diagram takes the system to a state $|j\rangle$. (Alternatively, the ground state may be composed of two states.) The anharmonic oscillation also involves two sets of diagrams describing single and double excitations of a single state, namely, two-level ($|0\rangle$ and $|1\rangle$) and three-level ($|0\rangle$, $|1\rangle$, and $|2\rangle$) diagrams. However, in the diagrams that produce the anharmonic oscillations, the first two interactions involve only the $|0\rangle$ and $|1\rangle$ states; there is no branching. In a quantum beat, the first interactions couple the ground and singly excited states of *two different modes,* but the emission occurs from the *singly excited state of a single mode.* In anharmonic oscillations, the first interactions involve ground and single excited states of *a single mode,* but the emission occurs from both *doubly and singly excited*

states of the same mode; the emission arises at the same frequency only because of inhomogeneous broadening.

The "two-level" diagrams, which have transitions only between the ground state and one of the two fundamentals, have a coherence between the $|0\rangle$ and $|1\rangle$ levels after the first pulse, that is, a density matrix element of $\rho_{01}(\omega)$ that evolves at frequency ω. The system interacts with the second pulse twice; the first interaction takes $\rho_{01}(\omega)$ into either $\rho_{00}(0)$ or $\rho_{11}(0)$ which have no phase evolution, and the second interaction takes both these elements into the $\rho_{10}(-\omega)$ coherence, which then evolves at frequency $-\omega$ (the negative frequency implies rephasing). The phase differences caused by inhomogeneous broadening that occurred in the time τ between the first and second pulse is rephased by time 2τ. Summing ω over all the frequencies in the inhomogeneous line produces a macroscopic polarization that dephases as a free induction decay (FID) after the first interaction, and that rephases and dephases again as an FID at a time τ after the second pulse, generating the echo pulse. One diagram involving the $|0\rangle$, $|1\rangle$, and $|2\rangle$ levels is responsible for the vibrational echo signal contribution from a 1-2 coherence. The density matrix elements corresponding to this diagram are $\rho_{00}(0) \rightarrow \rho_{01}(\omega) \rightarrow \rho_{11}(0) \rightarrow \rho_{21}(-(\omega - \Delta))$, where Δ is the anharmonic frequency shift of the 1-2 transition relative to the 0-1 transition and $\rightarrow$ represents an interaction with an E field.

The monochromator measures the signal from all oscillators emitting in a narrow bandwidth centered at frequency ω_o. There are two subensembles of molecules that can emit at ω_o. Molecules with $\rho_{10}(-\omega_o)$ (third interaction) and the corresponding $\rho_{01}(\omega_o)$ (first interaction) will emit at ω_o (two-level diagrams). Molecules with $\rho_{21}(-\omega_o)$ (third interaction) and the corresponding $\rho_{01}(\omega_o + \Delta)$ (first interaction) will also emit at ω_o (three-level diagram). The 1-2 transition frequency of this second set of molecules is at $(\omega_o + \Delta) - \Delta$; that is, their 0-1 transition frequency is $\omega_o + \Delta$, and the 1-2 emission frequency is redshifted by the anharmonic shift, Δ, bringing it to ω_o.

The frequency at which the oscillators emit, ω_o, is the frequency at which the oscillators rephase to form the echo pulse. In the diagrams involving only the $|0\rangle$ and $|1\rangle$ levels, the density matrix evolves as $\rho_{00}(0) \rightarrow \rho_{01}(\omega) \rightarrow \rho_{00}(0)$ [or $\rho_{11}(0)] \rightarrow \rho_{10}(-\omega_o)$. The two-level diagrams dephase and rephase at ω_o. In the diagram involving the $|0\rangle$, $|1\rangle$, and $|2\rangle$ levels, the situation is different. For a molecule with 0-1 transition frequency $(\omega_o + \Delta)$, the density matrix evolves as $\rho_{00}(0) \rightarrow \rho_{01}(\omega_o + \Delta) \rightarrow \rho_{11}(0) \rightarrow \rho_{21}\{-[(\omega_o + \Delta) - \Delta]\} = \rho_{21}(-\omega_o)$. Thus, the coherence produced by the three-level diagram dephases at $(\omega_o + \Delta)$ but rephases at ω_o, producing a polarization at ω_o. At τ, the time of the second pulse, there is a phase difference between $\rho_{01}(\omega_o)$ and $\rho_{01}(\omega_o + \Delta)$ equal to $\Delta \times \tau$. After the second pulse, both ensembles of oscillators begin rephasing at ω_o. Although the vibrational echo polarization produced by both types of diagrams have the same frequency, the two polarizations do not have the same phase. As τ is increased, the phase difference advances, giving rise to the oscillations in the "single" frequency detected signal. The analysis is identical for a three pulse stimulated vibrational echo. The oscillations can occur only when the first pulse can prepare a 0-1 coherence at both frequencies ω_o and $\omega_o + \Delta$; if the inhomogeneous linewidth is much smaller than the anharmonicity, then no oscillations will be detected at third order. The mechanism applies whether or not the echo is spectrally resolved. The oscillations come from the evolution of the phase relationship of two distinct subensembles of molecules that emit at the same frequency. Unlike a quantum beat, a branching transition is not involved in the first interaction, and, unlike a quantum beat, a sufficiently broad inhomogeneous line is required for the oscillation to occur.

Figure 2 presents calculations of the VES for a single anharmonic mode for two cases. Eight diagrams contribute to the signal detected in the phase matched direction; five of these are not rephasing diagrams, and contribute only

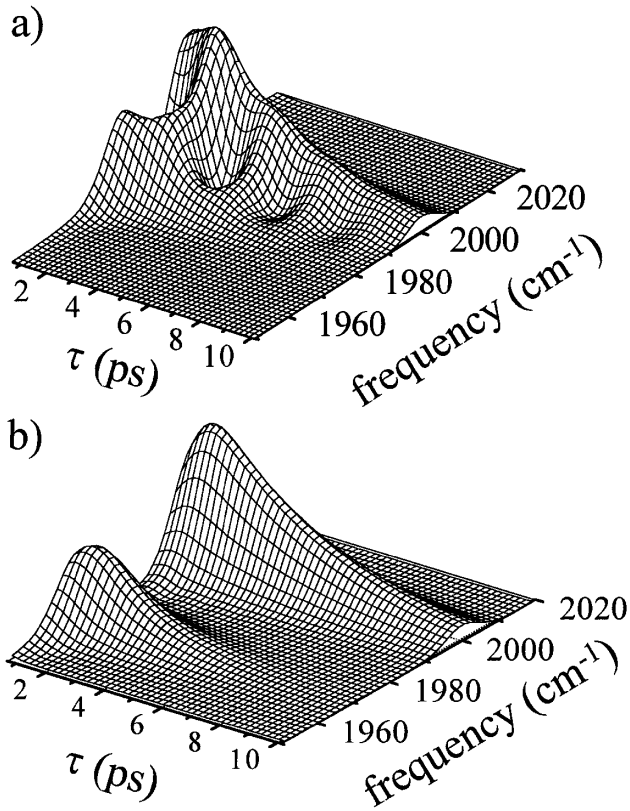

FIG. 2. Calculations of spectrally resolved VES data of a single mode for two situations. (a) The inhomogeneous linewidth is equal to the anharmonic shift. The 0-1 and 1-2 spectroscopic lines overlap, and oscillations occur at the anharmonic shift frequency. (b) The anharmonic shift is twice the inhomogeneous linewidth. The 0-1 and 1-2 transitions are well resolved, and there are no oscillations.

to the signal near $\tau = 0$. All eight terms have been included in the calculations. The calculated vibrational echo pulse for each delay time was Fourier transformed, and the one-sided power spectrum was computed. The 0-1 and 1-2 inhomogeneous lines were taken to have the same Gaussian inhomogeneous frequency distribution, and the anharmonicity is constant across the inhomogeneous line. Dephasing for each transition is taken to be exponentially damped. Figure 2(a) is for an inhomogeneous linewidth equal to the anharmonicity, and Fig. 2(b) is for an anharmonicity twice the inhomogeneous linewidth. Figure 2(a) resembles the antisymmetric mode data in Fig. 1(a). When the 0-1 and 1-2 inhomogeneous lines overlap [Fig. 2(a)], there are pronounced oscillations present at the anharmonic shift frequency. However, as can be seen from the figure, the blue side of the band yields the time dependence of the 0-1 transition, and the red side of the band yields the time dependence of the 1-2 transition. In a regular 1D vibrational echo decay (not spectrally resolved), there are oscillations and cross terms. Even if each transition has a distinct exponential decay, the resulting 1D curve is a triexponential with oscillations. If the decays are more complex than exponentials and the form is not known in advance [13], then without using this or other 2D methods reliable extraction of the dynamics of the individual transitions is virtually impossible. In Fig. 2(b), the two peaks are well resolved and show no oscillations. Without spectral resolution, the 1D decay for exponential damping would be a triexponential. With spectral resolution, the decays are isolated and there is no cross term. Thus, determination of the functional form of the vibrational dephasing is simplified with the 2D approach.

As shown in Fig. 1(b) and the inset, a quantum beat occurs between the A and S mode frequencies. The center-to-center splitting of the A and S modes is $\sim 71\ \mathrm{cm}^{-1}$. This is the nominal beat frequency for the quantum beats shown in the inset of Fig. 1(b). Three pairs of diagrams give rise to the beats. For example, for one pair the density matrix evolves as $\rho_{00}(0) \rightarrow \rho_{0A}(\omega_A) \rightarrow \rho_{AA}(0) \rightarrow \rho_{A0}(-\omega_A)$ and $\rho_{00}(0) \rightarrow \rho_{0S}(\omega_S) \rightarrow \rho_{00}(0) \rightarrow \rho_{A0}(-\omega_A)$, where the subscripts A and S stand for the first vibrational excited states of the A and S modes. The two paths dephase at different frequencies because distinct excited states are involved, but they rephase at the same frequency. This is a standard quantum beat that arises from a branching transition.

The experiments and theoretical calculations demonstrate that ultrafast 2D time-frequency IR vibrational echo experiments can extract a substantial amount of spectroscopic and dynamic information from complex molecular systems. The analysis presents an alternative interpretation for the anharmonic oscillations that is distinct from conventional quantum beats. For complex molecular systems, in which the 1D decay is a composite of the dynamics of many transitions, spectroscopically resolving the vibrational echo can greatly simplify data interpretation and make it possible to understand important molecular dynamical processes.

This work was supported by NIH (1RO1-GM61137), NSF (DMR-0088942), and AFOSR (F49620-94-1-0141).

[1] E. L. Hahn, Phys. Rev. **80**, 580 (1950).
[2] G. Bodenhausen, R. Freeman, G. A. Morris, and D. L. Turner, J. Magn. Reson. **31**, 75 (1978).
[3] N. A. Kurnit, I. D. Abella, and S. R. Hartmann, Phys. Rev. Lett. **13**, 567 (1964).
[4] W. P. deBoeij, M. S. Pshenichnikov, and D. A. Wiersma, Chem. Phys. **1998**, 287 (1998).
[5] S. M. Gallagher, A. W. Albrecht, T. D. Hybl, B. L. Landin, B. Rajaram, and D. M. Jonas, J. Opt. Soc. Am. B **15**, 2338 (1998).
[6] D. Zimdars, A. Tokmakoff, S. Chen, S. R. Greenfield, M. D. Fayer, T. I. Smith, and H. A. Schwettman, Phys. Rev. Lett. **70**, 2718 (1993).
[7] K. D. Rector, A. S. Kwok, C. Ferrante, A. Tokmakoff, C. W. Rella, and M. D. Fayer, J. Chem. Phys. **106**, 10 027 (1997).
[8] K. D. Rector, C. W. Rella, A. S. Kwok, J. R. Hill, S. G. Sligar, E. Y. P. Chien, D. D. Dlott, and M. D. Fayer, J. Phys. Chem. B **101**, 1468 (1997).
[9] K. D. Rector and M. D. Fayer, Int. Rev. Phys. Chem. **17**, 261 (1998).
[10] P. Hamm, M. Lim, W. F. Degrado, and R. M. Hochstrasser, J. Chem. Phys. **112**, 1907 (2000).
[11] M. C. Asplund, M. T. Zanni, and R. M. Hochstrasser, Proc. Natl. Acad. Sci. U.S.A. **97**, 8219 (2000).
[12] K. D. Rector, D. E. Thompson, K. Merchant, and M. D. Fayer, Chem. Phys. Lett. **316**, 122 (2000).
[13] M. A. Berg, K. D. Rector, and M. D. Fayer, J. Chem. Phys. **113**, 3233 (2000).
[14] J. D. Beckerle, M. P. Casassa, R. R. Cavanagh, E. J. Heilweil, and J. C. Stephenson, Chem. Phys. **160**, 487 (1992).
[15] K. D. Rector, M. D. Fayer, J. R. Engholm, E. Crosson, T. I. Smith, and H. A. Schwettmann, Chem. Phys. Lett. **305**, 51 (1999).
[16] K. D. Rector, D. A. Zimdars, and M. D. Fayer, J. Chem. Phys. **109**, 5455 (1998).
[17] W. M. Zhang, V. Chernyak, and S. Mukamel, J. Chem. Phys. **110**, 5011 (1999).
[18] M. C. Asplund, M. Lim, and R. M. Hochstrasser, Chem. Phys. Lett. **323**, 269 (2000).
[19] X. Yang and L. W. Jelinski, J. Magn. Reson. B **107**, 1 (1995).
[20] S. Mani, J. Pauly, S. Conolly, C. Meyer, and D. Nishimura, Magn. Reson. Med. **37**, 898 (1997).
[21] A. I. Lvovsky and S. R. Hartmann, Laser Phys. **6**, 535 (1996).
[22] M. Koch, J. Feldmann, G. von Plessen, E. O. Gobel, P. Thomas, and K. Kohler, Phys. Rev. Lett. **69**, 3631 (1992).
[23] P. Hamm, M. Lim, M. Asplund, and R. M. Hochstrasser, Chem. Phys. Lett. **301**, 167 (1999).